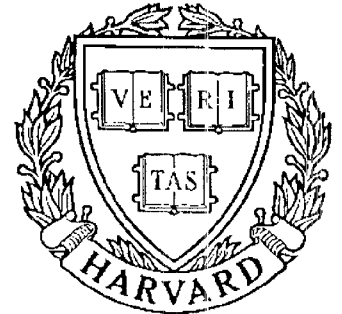


TECHNICAL RESEARCH REPORT



S Y S T E M S
R E S E A R C H
C E N T E R



*Supported by the
National Science Foundation
Engineering Research Center
Program (NSFD CD 8803012),
Industry and the University*

Analysis of the Cutting Dynamics in Microscale

by G.M. Zhang and T.W. Hwang

Analysis of the Cutting Dynamics in Microscale

G. M. Zhang and T. W. Hwang

**Mechanical Engineering Department and Systems Research Center
University of Maryland at College Park
College Park, MD 20742**

Abstract

This paper presents a new approach to the study of cutting dynamics in microscale. The manipulation of the cutting force generated during machining is based on the characteristics of microstructures within the workpiece material being machined. Mathematical modeling of the hardness variation around the circumference of the workpiece reveals the cohesiveness between the macroscale and microscale analyses. The case study presented in this paper illustrates the procedures used to evaluate the cutting force through the microscale analysis. A model-based indirect tool wear monitoring methodology has been developed to show the potential of applying the cutting dynamics in microscale for the design of on-line quality and process control systems.

1. Introduction

Cutting dynamics is a subject which deals with generation of the cutting force during machining. Dynamic variation of the cutting force is the major source of tool vibration. Researchers in the metal cutting community have made great efforts to explore the possibility of predicting the cutting force and its chain reaction with the structural dynamics of the machine tool.

As witnessed in the past, remarkable achievements in the study of cutting dynamics have been made. Since the introduction of Merchant's composite cutting force circle (Merchant, 1945), mathematical models have been developed for quantitative evaluations of the cutting force produced during various machining operations, such as turning, boring, milling, and grinding. The mathematical model proposed by von Turkovich (1972) revealed the thermoplastic characteristics of the rapid plastic deformation during machining. Tlustý (1978) summarized the state of research in cutting dynamics and suggested the directions of further research. The impact of these research achievements on manufacturing industries stimulates a historic evolutionary process to increase productivity and improve product quality through new machine tool designs and new cutting tools.

Due to the rapid advance in computer applications, production automation has undergone a new evolution to meet the challenges for higher productivity and better product

quality. New manufacturing technologies, such as on-line monitoring for quality control and implementation of computer-based untended machining (Koren, et al, 1987, and Tlustý and Andrews, 1983), have attracted great attention in the manufacturing community. Precision machining has been the focus of this endeavor. Industry is now concerned with tolerances on the order of a few micrometers. By comparison, tolerances of 10 to 100 micrometers were previously commonplace. Microscale characteristics of machined surfaces have become more important in the assessment of the functionality and reliability of the machined product. Consequently, analysis of the cutting dynamics in microscale has emerged as a new research area. Researchers hope that the dynamic variation of the cutting force generated during machining could be explained in microscale. The correlation between microscale and macroscale, regarding the cutting force variation, will provide a better understanding of the random tool motion during machining. Thus, a high machining accuracy may be obtained through effective control of said motion.

This paper presents a rational approach to the study of cutting dynamics in microscale. Starting from the shearing process in the cutting zone, the relation between cutting force generation and basic material properties, such as hardness, is studied. Through microstructural analysis of the workpiece material, this research reveals the mechanism of the cutting force variation due to the nonhomogeneous hardness distribution in the workpiece material. Considering the effect of the three cutting parameters (feed, depth of cut, and cutting speed) and the interaction between the cutting mechanism and the machine tool structure, this research bridges the gap between the microscale and the macroscale analyses and offers a quantitative evaluation of the dynamic cutting force generated during machining. The formulation of an on-line monitoring methodology is presented as an example to demonstrate how this research can be applied to practical quality control on the shop floor.

2. Analysis of Cutting Dynamics

2.1. General View of Cutting Force Generation

Common sense dictates that the cutting force is generated immediately after the cutting tool digs into the workpiece material. Metal shearing theories have been well accepted to explain cutting mechanics. As an initial approximation, the magnitude of the nominal cutting force is taken to be proportional to the cutting area, A_c , or the nominal chip load (a product of feed, f , and depth of cut, d), i.e.,

$$F_{\text{nominal}} = K_s A_c = K_s (f * d) \quad (1)$$

where the proportionality coefficient, K_s , is named as the unit cutting force. Results from empirical metal cutting research have already shown that the unit cutting force, K_s , is directly related to cutting conditions such as workpiece material, tool geometry, and the cutting parameters (feed, depth of cut, and cutting speed). For example, the unit cutting force for machining carbon steel ranges from 2000 Mpa to 2600 Mpa, while the unit cutting force for machining aluminum alloys is between only 700 Mpa and 900 Mpa. However, the unit cutting force can be treated as a constant under a specific set of known cutting conditions. Consequently, the cutting force evaluated based on Equation (1) is called the nominal cutting force.

The cutting force generated during machining is a vector quantity and thus possesses its own distinct direction. This direction plays an important role in the determination of machining performance. As a typical example, one might utilize a negative rake angle to maintain a compressive stress field in a carbide tip tool in an attempt to control the cutting force direction to avoid tool breakage. There has been substantial research on the determination of shear angle in the cutting zone, both analytically and experimentally.

It should be pointed out that the evaluation of the generated cutting force in the previous research is on a macroscale. It is a common practice that the cutting force is formulated as a function of basic properties of the workpiece material (hardness and ductility), cutting parameters (feed, depth of cut, and cutting speed), and tool geometry. For overlapping cuttings, the surface modulation fed back through the regenerative mechanism to the cutting zone adds more dynamic variation to the cutting force. However, this variation is also dealt with on a macroscale. The cutting dynamics in macroscale address stability of the machining system, the transient response of tool vibration, and the determination of the dynamic equilibrium position of the cutting tool. However, an inefficiency associated with the macroscale analysis of cutting dynamics is its failure to explain random tool motion observed during machining. This is due to the absence of any analytical ground to support the establishment of a random excitation system capable of describing random tool vibration. As a result, there exists a pressing need to advance the study of cutting dynamics. One important aspect is to extend the cutting dynamics from the current macroscale study to a microscale study, thus forming a scientific basis for the evaluation of random tool motion.

2.2. Basic Assumptions

Research of the cutting dynamics in microscale has already been carried out as far back as a century ago. The photomicrograph of a partially formed chip confirmed the

assumption that metal undergoes shearing strain in the cutting zone. Further study of cutting dynamics comes from today's need for better control of machining accuracy. People have realized that a preheat-treatment, which alters characteristics of microstructures within the workpiece, may improve machinability of the workpiece material significantly. Also, proper selection of cutting data such as feed, depth of cut, and cutting speed seems to be an effective means to assure a high level of machining quality while maintaining high productivity. For quality control in automation, on-line monitoring of the machining process or the tool wear progress has been proposed and implemented on the machine tool design to reduce defects on a real-time basis. A key to the success of such monitoring systems is true detection of process deterioration. This requires human intervention or services. Since natural process variation is always present during machining, for on-line monitoring systems to effectively detect deterioration and avoid false alarming, the separation of process deterioration, such as tool wear, from such natural variation is made essential. This requires integration of a quantitative prediction of the natural process variation and a statistical inference of the deterioration. The evaluation of random tool motion serves as a basis in this regard.

As a preliminary study for the cutting force evaluation in microscale, the following two assumptions are made.

1. The major cause of random variation of the cutting force during machining is the nonhomogeneous hardness distribution of the material being machined.
2. The random variation of the cutting force is mainly embodied in the variation of the magnitude of the cutting force. Thus, the direction of the cutting force remains unchanged or the directional changes due to the nonhomogeneous hardness distribution are too small to be of consequence.

It is already known that several factors, such as built-up edges, tool wear, and material hardness variation, are related to the random variation of the cutting force. The first assumption narrows our discussion to a cutting speed range. If only relatively high cutting speeds are considered, the effect of built-up edges on the cutting force variation may be neglected. Tactically, tool wear is treated as a process deterioration factor to be detected in an on-line monitoring system. Thus, its effect on the cutting force variation need not be counted in the present study. The effect of the material hardness variation on the cutting force variation is considered to represent the natural variation of machining accuracy.

To validate the second assumption, the friction force between the chip and tool rake face in the second deformation zone is believed to dominate the determination of the direction of cutting force. Factors related to the friction force are: chemical compositions of the workpiece and tool insert materials, cutting temperature, and tool geometry. The

material hardness variation can hardly be related to the friction force variation. Consequently, the material hardness variation also may not be related to the variation of the cutting force direction.

2.3 Cutting Force Evaluation in Microscale

Figure 1 presents an enlarged view of a machining configuration taken from a single-point turning process. The outside layer will be removed after one revolution of the workpiece. In microscale, it may be imagined that the tool meets microstructures along its cutting edge instantaneously. The difference between the constituents of the microstructures removed by the cutting edge at two instants can be anticipated. A technique to take this measurement would be of great value since it would enable the evaluation of the instantaneous cutting force.

A statistical approach was proposed in an effort to mathematically describe the phenomenon of random variation of the cutting force generation. This approach is comprised of three procedures:

1. Microstructural analysis of the material to be machined.
2. Identification of random excitation during machining.
3. Establishment of the relationship between the three cutting parameters (f , d , v) and random variation of the cutting force.

2.3.1 Microstructural Analysis

In order to quantify the effects of basic material properties, such as microhardness variation on the cutting force generation, metallurgic identification of the microstructures present in the material is essential. In this research, a representative sample of the material to be machined (SAE 1015) is taken. Figure 2a presents the image taken directly from the sample. Figure 2b presents the same image after contrast enhancement to identify the type of microstructures at each location in the sample. After measuring the microhardness value for each identified microstructure, the three statistics, μ_a , σ_a^2 , and $\rho(r)$, may be calculated.

$$\mu_a = \frac{1}{N} \sum_{i=1}^N H_i \quad (2)$$

$$\sigma_a^2 = \frac{1}{N} \sum_{i=1}^N (H_i - \mu_a)^2 \quad (3)$$

$$\rho(r) = \frac{\sum_{i=1}^N (H_i - \mu_a)(H_{i'} - \mu_a)}{N\sigma_a^2} \quad (4)$$

where N = number of locations taken on the chosen representative part.
 H_i = microhardness value at the i^{th} location.
 r = $|i - i'|$, the distance in space between points i and i' .

In general, μ_a represents the average hardness value of the material to be machined, σ_a^2 indicates the level of hardness variation from point to point within the material, and $\rho(r)$

is the correlation coefficient function which provides quantitative information on size, shape, and segregation of the microstructures present in the material. The two curves shown in Figure 3 are plots of two correlation coefficient functions. The solid line curve is the correlation coefficient function $\rho(r)$ calculated from the microstructure distribution shown in Fig. 2b (before heat treatment). The dashed line curve is the correlation coefficient function calculated from the microstructure distribution after a spherized heat treatment. A sharp decrease shown in the dashed line curve indicates small sizes and spherical shapes of the microstructures after the heat treatment.

2.3.2. Random Excitation Model

Upon identifying the characteristics of the hardness variation in microscale, the second procedure is performed to relate this information to random tool motion. As illustrated in Fig. 1, the volume of the workpiece material removed during any time interval, Δt , may be considered to be equal to the volume of a parallelepiped. As indicated in Fig. 1, the cross-sectional area of this parallelepiped is equal to the product of feed and depth of cut. The height of this parallelepiped is given by

$$\frac{\pi D}{n} = \frac{\pi D}{T/\Delta t} = \frac{\pi D \Omega \Delta t}{60} \quad (5)$$

where D is the diameter of the workpiece, T is the time needed for one revolution of the workpiece, Ω is the rotational speed of workpiece in rpm, and n , equivalent to $T/\Delta t$, is the number of parallelepipeds assumed along the circumference of the workpiece. Due to the nonhomogeneous distribution of microstructures, the microstructural constituents within individual parallelepipeds are distinct from one another. Averaging the microhardness values for each parallelepiped and taking this averaged value as an index to represent the parallelepiped hardness value, averaged hardness values of $\mu_1, \mu_2, \dots, \mu_n$ at time instants

$\Delta t, 2\Delta t, \dots n\Delta t$, respectively, may be obtained. For those μ_i 's larger than $\bar{\mu}$, the mean value of $\mu_1, \mu_2, \dots \mu_n$, it is expected that the cutting force magnitudes at the corresponding time instants are larger than the nominal cutting force, and vice versa. As a result of the introduction of the ratio term, $\frac{\mu_i}{\mu}$, to Equation (1), the effect of the nonhomogeneous hardness distribution into the cutting force evaluation may be accounted for at time instants $\Delta t, 2\Delta t, \dots n\Delta t$, respectively.

$$F_{\text{resultant}} = K_s A_c \left[\frac{\mu_i}{\mu} \right]^m \quad i = 1, 2, \dots n \quad (6)$$

where the exponent "m" in Equation (6) explains the nonlinear relation between the instantaneous cutting force and the hardness ratio term, $\frac{\mu_i}{\mu}$. If we separate the nominal cutting force from the resultant cutting force, the remainder represents the random variation of the cutting force. This decomposition is given by

$$F_{\text{resultant}} = F_{\text{nominal}} + F_{\text{random}} = K_s A_c + K_s A_c \left\{ \left[\frac{\mu_i}{\mu} \right]^m - 1 \right\} \quad i = 1, 2, \dots n \quad (7)$$

Equation (7) allows the simulation of downward to upward, or vice versa, changes in the magnitude variation of the cutting force. A large "n" value, which corresponds to a small height value of the parallelepiped, is related to high frequency components of the cutting force. The highest frequency, f_{max} , of the cutting force variation which can be represented by Equation (7) is given by

$$f_{\text{max}} = \frac{T/\Delta t}{2} \frac{\Omega}{60} = \frac{n}{2} \frac{\Omega}{60} \quad (\text{Hz}) \quad (8)$$

The relation between the three cutting parameters and the random variation of the cutting force can be sensed from the fact that a large parallelepiped volume reduces the variation of microstructural constituents within individual parallelepipeds. As illustrated in Fig. 1, it is evident that increasing feed or/and depth of cut adds an additional volume to the parallelepiped. Consequently, the random variation of the cutting force is reduced due to the reduced variation of microstructural constituent contents within the parallelepipeds. Quantitative relations between the three cutting parameters and the random variation of the cutting force have been established by Zhang (1986).

$$\sigma^2 = 4\pi\sigma_a^2 \left(\frac{n}{f d v}\right) \int_{r=0}^{\infty} \rho(r) W(r) r^2 dr \quad (9)$$

and

$$\sigma^2 = \frac{1}{n} \sum_{i=1}^n (\mu_i - \bar{\mu})^2 = \frac{1}{n} \sum_{i=1}^n (\mu_i - \mu_a)^2 \quad (10)$$

where $W(r)$ is called the geometric parallelepiped shape function. It is clear that parameters such as μ_a and σ_a^2 in Equations (9) and (10) are determined through microstructural analysis, while the parameters μ_s , $\bar{\mu}$, and σ^2 are defined in the macroscale. Therefore, integration of Equations (6), (9), and (10) in the cutting force evaluation bridges the gap between the macroscale and microscale analyses.

2.3.3 Interaction between the Cutting Mechanism and Machine Tool Structure

As evidenced from Figure 1, tool vibration changes the nominal chip load instantaneously (the primary feedback path) and the surface modulation produced behind will also alter the nominal chip load during the succeeding revolution of the workpiece under overlapping cutting (the regenerative feedback path). The two dynamic variations of the chip load inevitably lead to the dynamic variation of the cutting force, i.e.,

$$F_{\text{primary}} = -K_s w [a - y(t)] \quad (11)$$

$$F_{\text{regenerative}} = K_s w [\nu y(t-T)] \quad (12)$$

where "w" is the width of cut, "a" is the thickness of cut, ν is the overlapping factor, $y(t)$ is the instantaneous position of the tool or the system response, and $y(t-T)$ is the thickness of the uncut part during the preceding revolution of the workpiece.

From an analytical point of view, the cutting force generated during machining should consist of four components i.e.,

$$\begin{aligned} F_{\text{resultant}} &= F_{\text{nominal}} + F_{\text{random}} + F_{\text{primary}} + F_{\text{regenerative}} \\ &= K_s A_c \left[\frac{\mu_s}{\mu_a} \right]^m - K_s w [a - y(t)] + K_s w [\nu \Delta y(t-T)] \end{aligned} \quad (13)$$

In the case of nonoverlapping cutting, the fourth component diminishes. It is evident that the evaluation of F_{primary} and $F_{\text{regenerative}}$ is heavily dependent upon the dynamic characteristics of the machine tool structure. This indicates the interaction between the cutting mechanism and the structural dynamics of the machine tool during machining.

The Merritt block diagram shown in Fig. 4 explicitly illustrates the chain reaction (Merritt, 1965). The input to the cutting mechanism consists of the chip load and the output is the cutting force. Additionally, the cutting force serves as the input to the structural dynamics of the machine tool for which the tool vibratory motion is the output. This vibratory motion in turn changes the chip load through the primary and regenerative feedback paths. Note the symbol of a normal distribution displayed in Fig. 4. This symbol represents the incorporation of the random excitation system to the cutting force evaluation through the cutting dynamics in microscale.

4. Computer Simulation

To demonstrate the essential experimental and analytical procedures for the study of cutting dynamics in microscale, this paper presents a case study. During this study, the instantaneous cutting force is manipulated during the first four revolutions of the workpiece on a lathe. Computer simulation has been carried out based on the Merritt block diagram shown in Fig. 4. The following parameters were used.

- | | |
|--|---|
| 1. Workpiece material: | SAE 1015 |
| 2. Workpiece geometry: | Length x Diameter = 500 x 200 mm |
| 3. Tool geometry: | Nose radius = 0.8 mm and rake angle = 0° |
| 4. Cutting data: | feed = 0.10 mm/rev, depth of cut = 0.6 mm |
| 5. Spindle Speed: | 600 rpm |
| 6. Unit cutting force: | 2000 Mpa |
| 7. Structural Dynamics
of the Lathe
(one-degree-of-freedom): | stiffness = 1×10^6 N/m
damping ratio = 0.05
equivalent mass = 2 kg |

For the random excitation model, $\mu_a = \overline{\mu} = 154$ (BHN) and $\sigma^2 = 180$ (BHN²) are assumed based on the correlation coefficient function $\rho(r)$ shown in Fig. 3 (solid line). The number of parallelepipeds on the circumference is taken as $n = 100$, which is equivalent to $f_{\max} = 500$ Hz.

Figure 5 presents the simulation result. As indicated in Fig. 5a, the nominal cutting force is constant. Its numerical value is equal to $K_s (f * d) = 120$ Newtons. The random variation of the cutting force is shown in Fig. 5b. The random changes of magnitude of this cutting force component represent the cutting edge meeting hard spots or soft spots in a random fashion during machining. The maximum variation is about 15% of the nominal cutting force. Figure 5c shows the cutting force variation due to the chip load variation

through the primary feedback path. Upon careful examination of this variation, a shift of the mean level and the variation about the mean level may be observed. The shift of the mean level corresponds to the shift from the static equilibrium of the tool (the tool set position prior to machining) to the tool dynamic equilibrium due to the presence of the nominal cutting force during machining. The variation of this component decays as a result of the cutting tool presumably reaching, and staying at, its dynamic equilibrium position. The dynamic variation of the cutting force shown in Fig. 5d is due to the presence of the residual chip load through the regenerative feedback path. As indicated in Fig. 5d, there is no variation during the first revolution of the workpiece simply because the residual chip load does not exist during the first revolution. The variation shown in Fig. 5d is about 6% of the nominal cutting force. The instantaneous cutting force generated during machining, which is shown in Fig. 5e, is a sum of these four components. A careful examination of the instantaneous cutting force reveals that the dynamic variation of the instantaneous cutting force is contributed mainly by both the cutting mechanism and the interaction between the cutting mechanism and the structural dynamics of the machine tool. This confirms the conclusions drawn by other researchers (Kegg, 1965 and Tlustý 1978) that the cutting process and machine tool are the two basic linked elements of the closed chatter loop. As shown in Fig. 5e, the impact between the tool and workpiece at the beginning of machining affects the instantaneous cutting force significantly. However, the transient process attenuates rapidly. This indicates that the random excitation phenomenon dominates the dynamic variation of the instantaneous cutting force when the machining process reaches steady state. This fact clearly demonstrates the importance of the study of cutting dynamics in microscale for the purpose of cutting force evaluation.

5. Application in On-Line Monitoring of Tool Wear

Common sense dictates that cutting dynamics plays an important role in machining chatter. To demonstrate the significance of studying the cutting dynamics in microscale, the design of an indirect on-line tool wear monitoring system, which relies on the analytical background from the cutting dynamics in microscale, is presented.

The objective of such a monitoring system is to control the tool wear progress during machining. When the tool wear rate reaches a certain critical value, human service should be called in to replace the worn tool to avoid an undesirable machining operation. As a result of the difficulties encountered in accessing the tool wear zones during machining, direct on-line tool wear sensing methods, have not been successful in shop floor applications in terms of cost and effectiveness, although they have been reported in use (Cook, N.H. and Subramanian, K., 1978). On the other hand, indirect on-line tool

wear sensing methods have been proposed (De Filippi, A. and Ippolito, R., 1969, and Pandit, S.M. and Kashou, S., 1982). Those methods depend upon reliable on-line signal detection, such as on-line cutting force measurement. Additionally, they retrace the tool wear progress based on the correlation between the tool wear mechanism and the dynamic variation of the on-line detected signal.

5.1 On-Line Monitoring Strategy

This approach in the design of such an on-line tool wear monitoring system has its own uniqueness.

1. A machining performance index, or indices, is defined to quantify the objective of designing the required on-line monitoring system. For demonstration purposes, it is assumed that the surface roughness characterization index - roughness average, R_a , is chosen as the machining performance index. A desirable machining operation is quantitatively characterized by allowing measurements of R_a taken from the machined surface to be below a certain quantitative limit.
2. The concept used in traditional statistical quality control methods, i.e., any production process is associated with a certain level of the performance variation called the natural performance variation, is employed. One of the major tasks in quality control is to identify the cause, or causes, which deteriorates the process performance through the introduction of additional performance variations to the natural performance variation.
3. The natural performance variation associated with the R_a measurement is observed to come from two resources. The first of these resources is the tool vibratory motion due to the dynamic variation of the cutting force. The second resource is due to the location where a trace is taken during the R_a measurement. Surface profiles taken from different locations on the machined surface are not identical in geometrical shapes. Such a variation among the R_a measurements is unavoidable.
4. The effect of tool wear on the machining performance index, R_a , is treated as an external cause which introduces an additional performance variation to the machining operation. This is as a result of the well known fact that excessive roughness often indicates that the tool has become worn (Lovett, 1989). As long as the tool wear rate stays at levels such that the R_a measurement is below the critical value, the monitoring system should leave the machining process unaltered. Otherwise, the monitoring system should call upon human intervention for tool replacement.

5.2. Construction of Control Chart

The results obtained from the study of the cutting dynamics in microscale have provided a useful tool for the design of such an on-line monitoring system outlined above.

1. Through microstructural analysis of the material to be machined, a random excitation model may be readily available to represent the random variation of the cutting force. By assuming that a machining system model is available, the application of the dynamic cutting force to the machine tool structure for the evaluation of the tool vibratory motion is possible. By combining the tool spiral trajectory path with the tool vibratory motion in a synchronous manner, the position of the cutting part of the tool may be retraced instantly. This allows the construction of the surface texture formed during machining. The surface topography shown in Fig. 6 is taken from a recent publication (Zhang, et al., 1990). The main theoretical background to support this construction is the cutting dynamics in microscale.
2. As a result of the availability of the numerical database of topography information, prediction of the R_a value from the surface profiles displayed in the constructed topography is possible, rather than having to take traces from the machined surface. Assuming that $R_{a1}, R_{a2}, \dots, R_{a99}, R_{a100}$ are the R_a values calculated at 100 different locations on the simulated surface topography, two relations may be obtained.

$$R_{a\text{-mean}} = \frac{1}{100} [R_{a1} + R_{a2} + \dots + R_{a99} + R_{a100}] \quad (14)$$

$$\sigma_{R_a}^2 = \frac{1}{100} \sum_{i=1}^{100} (R_{ai} - R_{a\text{-mean}})^2 \quad (15)$$

These two parameters characterize the mean and variation of the R_a measurements. They provide quantitative information about the natural performance variation and form a basis for the construction of $\overline{R_a}$ - and σ_{R_a} - charts. For demonstration purposes, a constructed $\overline{R_a}$ - chart is shown in Fig.

7, where the sample size = 5 and $3\sigma/\sqrt{5}$ principle are assumed.

3. The block diagram shown in Fig. 8 outlines the methodology to perform an on-line monitoring based on the signal detection of cutting force. Assume that the cutting force signals are recorded at regular time intervals, such as $F_1(t), F_2(t + T), F_3(t + 2T) \dots F_i(t + (i-1)T)$, where T is the time needed for one revolution of the workpiece. A computer vision of the surface profile, which is depicted in

Fig. 9, may be obtained. In fact, a series of R_a values may be calculated from this surface profile. However, the same cut-off value as the cut-off value used in the determination of $R_{a1}, R_{a2}, \dots, R_{a99}, R_{a100}$ must be maintained.

In order to utilize the constructed $\overline{R_a}$ - chart, a concept of moving average is introduced to calculate individual values of $\overline{R_{ai}}$ in the following way.

$$\begin{aligned}\overline{R_{a1}} &= \frac{1}{5} [R_{a1} + R_{a2} + R_{a3} + R_{a4} + R_{a5}] \\ \overline{R_{a2}} &= \frac{1}{5} [R_{a2} + R_{a3} + R_{a4} + R_{a5} + R_{a6}] \\ &\dots\dots\dots \\ \overline{R_{ai}} &= \frac{1}{5} [R_{ai} + R_{a(i+1)} + R_{a(i+2)} + R_{a(i+3)} + R_{a(i+4)}]\end{aligned}$$

Comparing the above $\overline{R_{a1}}, \overline{R_{a2}}, \dots, \overline{R_{ai}}$ with the upper and lower limits, or plotting the above $\overline{R_{a1}}, \overline{R_{a2}}, \dots, \overline{R_{ai}}$ on the $\overline{R_a}$ - chart against the upper and lower limits, the on-line monitoring system is capable of tracking the tool moving path. As long as the monitored values of $\overline{R_{ai}}$ do not exceed the control limits and display a normal variation pattern about the center line of the control chart, no human intervention is needed. When an abnormal situation occurs on the control chart, for example one $\overline{R_{ai}}$ value exceeds the upper limits, the on-line monitoring system will signify the warning alert indicating that the finish quality of the machined surface being machined has been deteriorated and human service is needed to restore the machining operation back to a normal status.

In fact, this proposed on-line tool wear monitoring system can be further improved by preparing a multi-stage control chart. According to different stages of tool wear rate, corresponding sets of the upper and lower limits may be established. When a new tool is being used after replacement, the on-line monitoring system checks the detected signal with the different control limits to provide additional information about the tool wear progress during machining.

6. Conclusions

1. This paper presents a preliminary study of cutting dynamics in microscale. The plastic shearing action in the cutting zone has a definite relation with the characteristics of microstructures within the workpiece material being cut. By combining the chip formation mechanics and the interaction between the cutting process and the structural dynamics of the machine tool, the instantaneous cutting force has been evaluated through evaluation of its four components. These

components are related to: the nominal chip load, random excitation, primary feedback path, and regenerative feedback path under overlapping cutting, respectively. Such an evaluation of the dynamic cutting force forms the basis for an accurate prediction of the tool motion during machining, representing a consequential progress in the scientific metal cutting research.

2. The basic procedures to study the cutting dynamics in microscale are microstructural analysis, formulation of the random excitation, and evaluation of the instantaneous cutting force through computer simulation. They follow a well defined evolutionary path in metal cutting research. As demonstrated in the case study, this work is capable of providing a practical approach to estimate natural process variation in terms of the finish quality of machined surfaces. Such information is vital to the development of an on-line tool wear monitoring system which would retrace the tool wear progress through an indirect on-line signal detection.
3. Other potential applications of this research are in the area of off-line optimization of machining. The proposed methodology can support the decision-making process of selecting cutting parameters such as feed, depth of cut, and cutting speed by comparing the simulation results with the specifications on a blue print. Such a capability meets the increasing demand in machining operation planning, especially in NC machining where the selection of the cutting specifications has to be made during the programming stage.

Acknowledgements

The authors acknowledge the support of the Systems Research Center at the University of Maryland at College Park under Engineering Research Centers Program: NSFD CDF 8803012. They wish to thank Professor W. L. Fournery, Chairman of the Mechanical Engineering Department, for his valuable support in conducting this work. They also thank Mr. J. Feldstein for his assistance in the preparation of this manuscript.

References

1. Cook, N.H. and Subarmanian, K., "Micro-Isotope Tool Wear Sensor," Annals of the CIRP, Vol. 27, 1978, pp. 73-78.

2. De Filippi, A. and Ippolito, R., "Adaptive Control in Turning: Cutting Forces and Tool Wear Relationships for P10, P20, P30 Carbides," *Annals of the CIRP*, Vol. 17, 1969, pp. 377-379.
3. Kegg, R. L., "Cutting Dynamics in Machine Tool Chatter," *Journal of Engineering for Industry*, ASME Trans., Vol. 87, 1965, pp. 464-470.
4. Koren, Y., Danai, K., Ulsoy, A.G., and Ko, T.R., "Monitoring Tool Wear Through Force Measurement," *Proceedings of the 15th North American Manufacturing Research Conference*, Vol. 2, 1987, pp. 463-468.
5. Kronenberg, M., "Machining Science and Application," Pergamon Press Inc., 1966.
6. Lovett, C.D., "Progress Report of the Quality in Automation Project for FY88," NISTIR 89-4045, National Institute of Standards and Technology, April 1989.
7. Merchant, M.E., "Mechanics of the Metal Cutting Process - Orthogonal Cutting and a Type - 2 Chip," *Journal of Applied Physics*, Vol. 16, No. 5, 1945, pp. 267-275.
8. Merritt, H. E., "Theory of Self-Excited Machine-Tool Chatter," *Trans. ASME*, Vol. 87, November 1965, pp. 447-454.
9. Pandit, S.M. and Kashou, S., "A Data Dependent Systems Strategy of On-Line Tool Wear Sensing," *Journal of Engineering for Industry*, ASME Trans., Vol. 104, 1982, pp. 217-223.
10. Peklenik, J. "Investigation of the Surface Typology," *Annals of the CIRP*, Vol. 15, 1967, pp. 381-385.
11. Tlustý, J., "Analysis of the State of Research in Cutting Dynamics," *Annals of the CIRP*, Vol. 27/2/1978, pp. 583-589.
12. Tlustý, J. and Andrews, G.C., "A Critical Review of Sensors for Unmanned Machining," *Annals of the CIRP*, Vol. 32/2/1983, pp. 563-572.
13. Villa, A., Rossetto, S., and Levi, R., "Surface Texture and Machining Conditions, Part1: Model Building Logic in View of Process Control," *ASME Trans., Series B*, Vol. 105, No. 4, 1983, pp. 259-263.
14. von Turkovich, B.F., "On a Class of Thermomechanical Processes during Rapid Plastic Deformation," (with special reference to metal cutting), *Annals of the CIRP*, Vol. 21, No. 1, 1972, p. 15.
15. Zhang, G.M., "Dynamic Modeling and Dynamic Analysis of the Boring Machining System," Ph.D. Thesis, University of Illinois at Urbana-Champaign, 1986.
16. Zhang, G.M., Hwang, T.W., and Harhalakis, G., "Control of Surface Topographies Formed during Machining," *Proceedings of the Second International Conference on Computer Integrated Manufacturing*, May 1990.

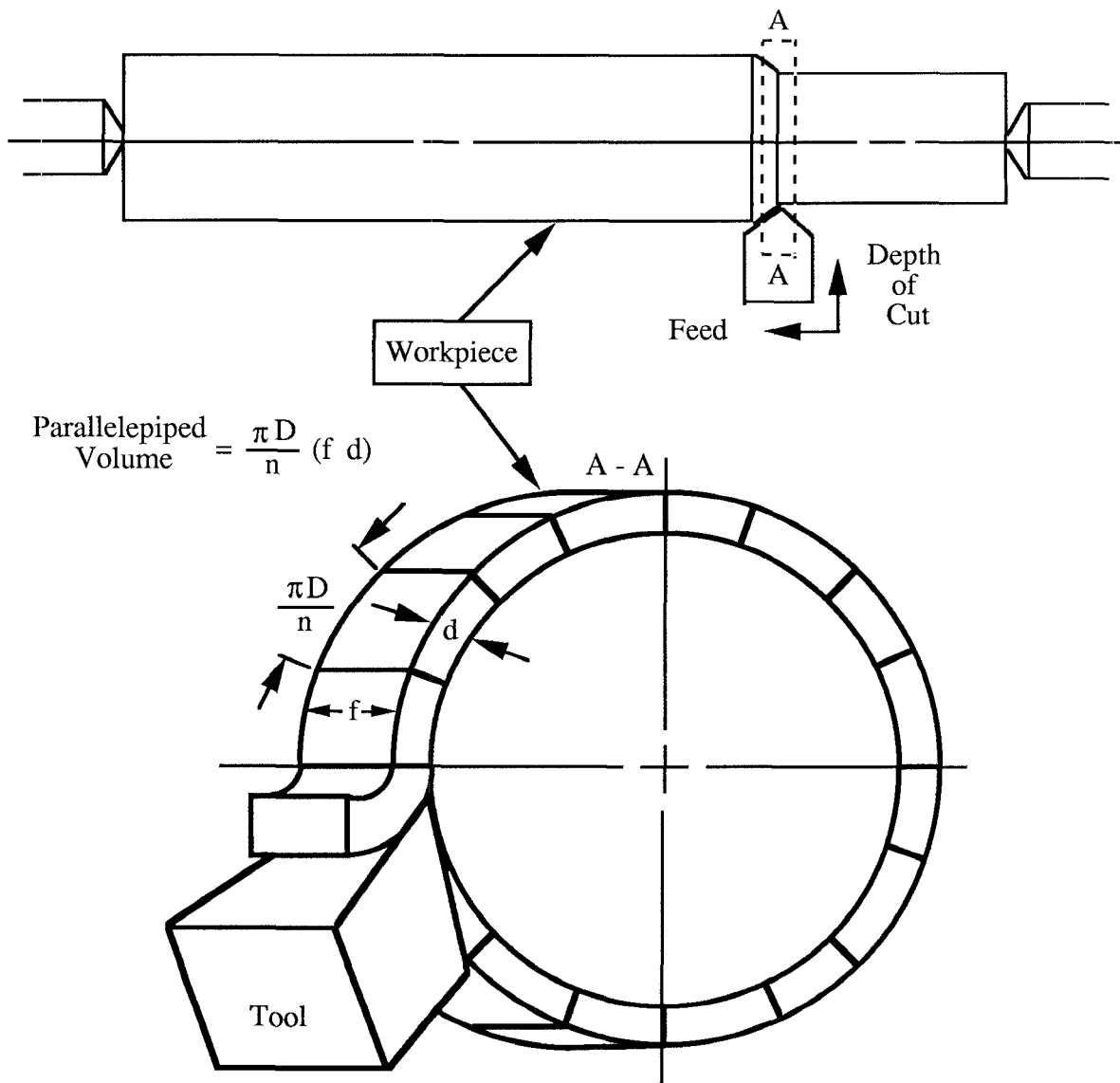
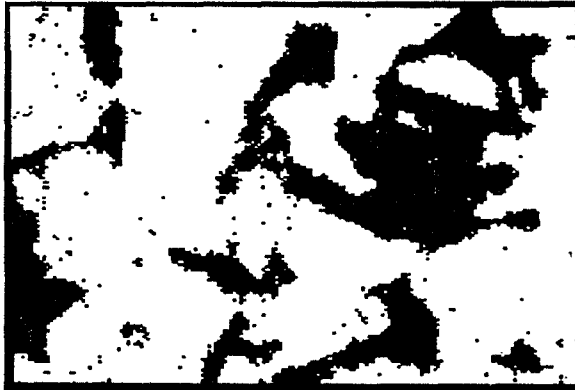


Figure 1 Enlarged View of a Single-Point Turning Process



(a) Sample Image Taken from Specimen
(before Contrast Enhancement)



(b) Sample Image Taken from Specimen
(after Contrast Enhancement)

Fig. 2 Experimental Microstructural Analysis

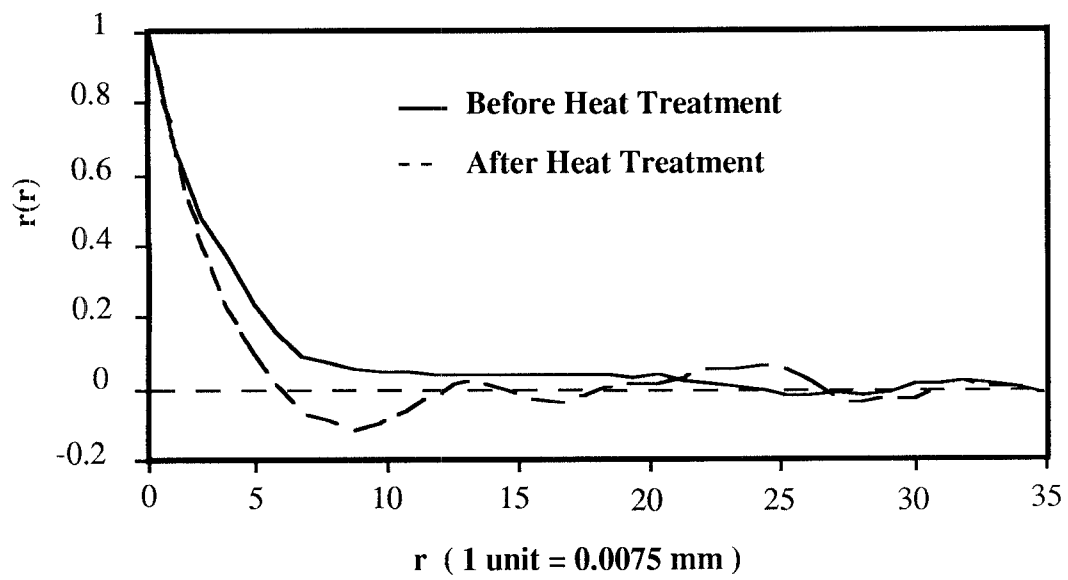


Figure 3 Correlation Coefficient Functions

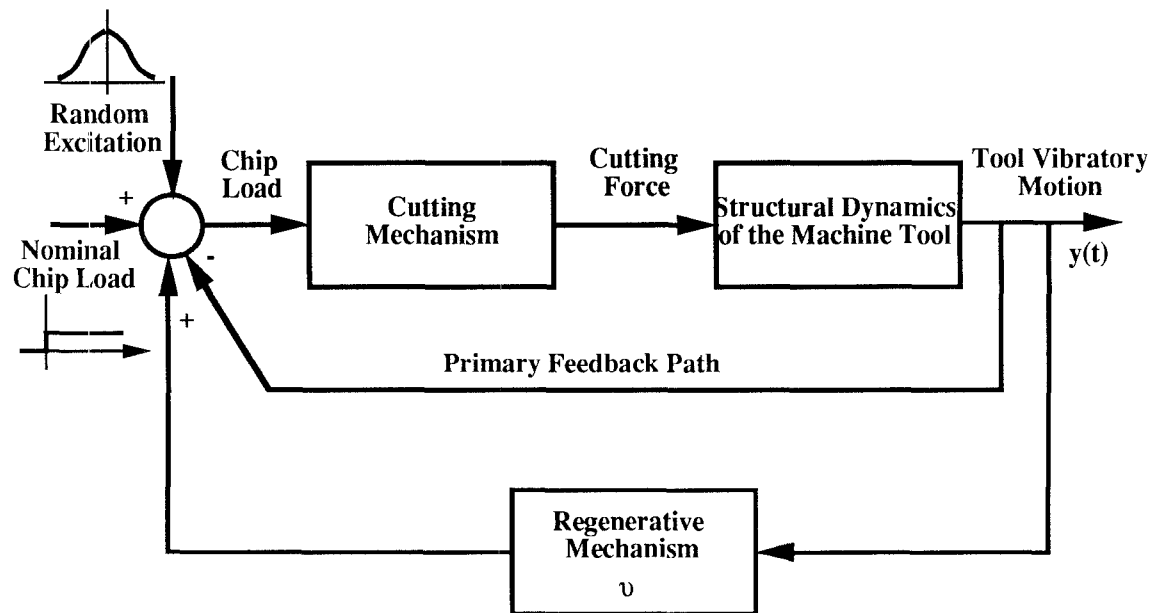
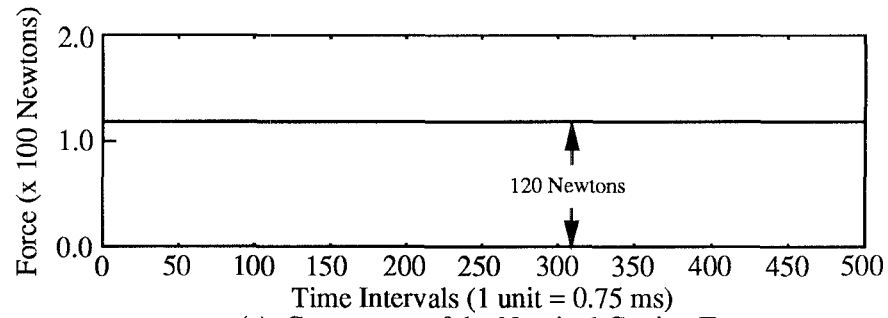
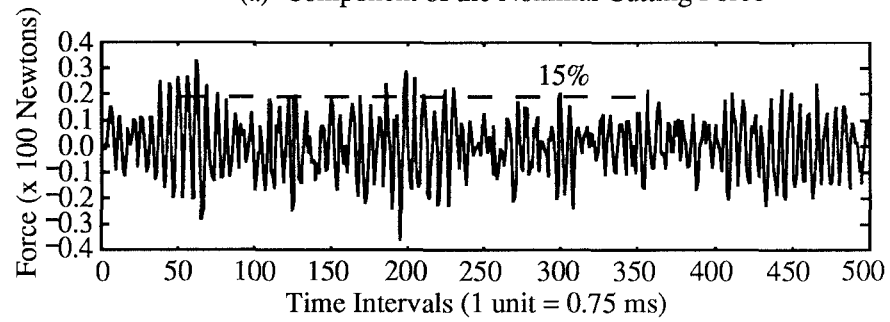


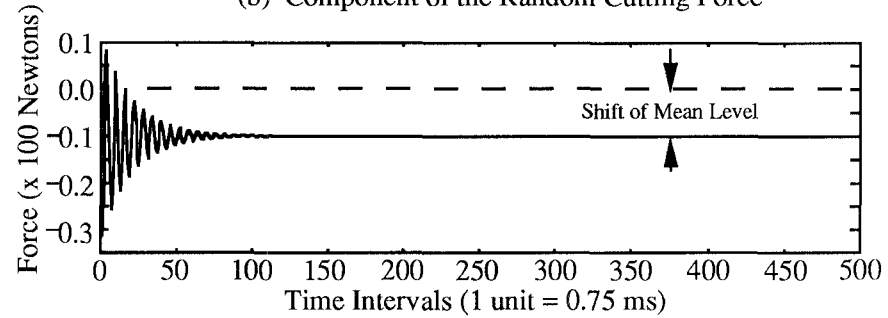
Fig. 4 Merritt Block Diagram Representing the Machining System



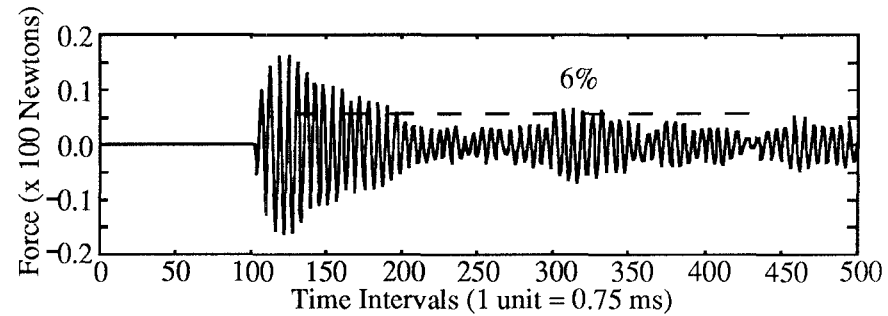
(a) Component of the Nominal Cutting Force



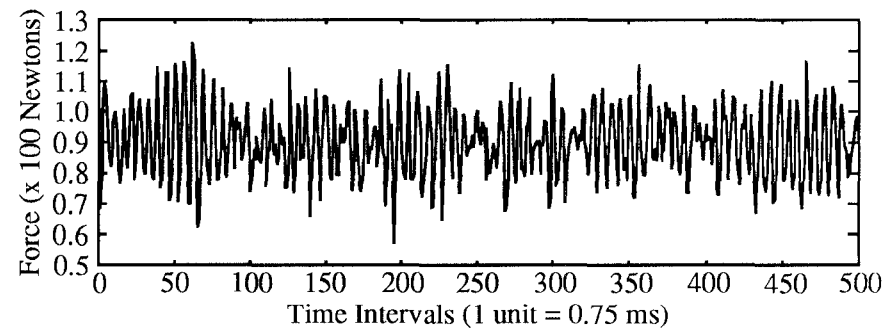
(b) Component of the Random Cutting Force



(c) Component Contributed by the Primary Feedback Path

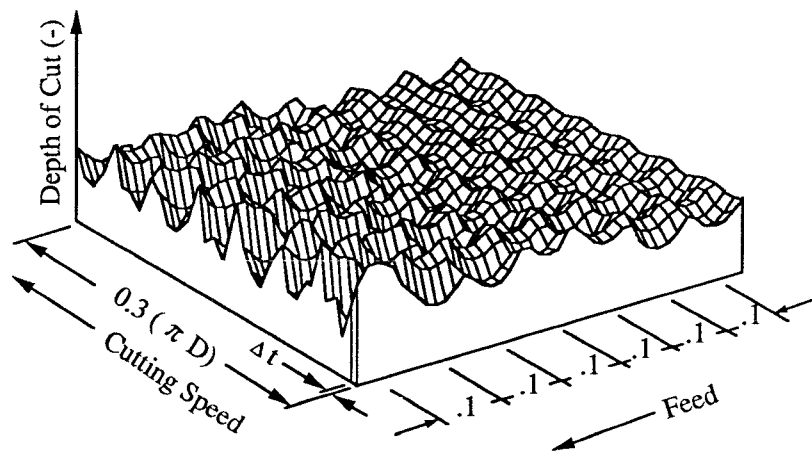


(d) Component Contributed by the Regenerative Feedback Path



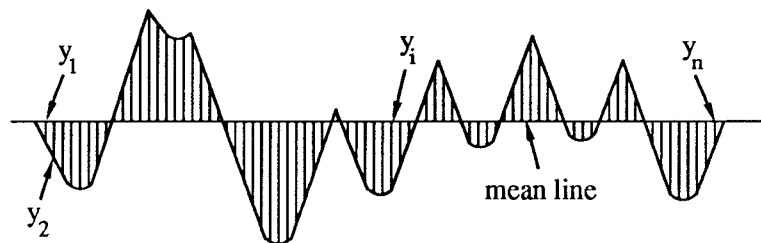
(e) Instantaneous Cutting Force Generated during Machining
(Sum of the Four Cutting Force Components)

Figure 5 Cutting Force Analysis



Surface Roughness $R_{a \text{ mean}} = 3.4 \mu\text{m}$

Standard Deviation $\sigma_{R_a} = 1.8 \mu\text{m}$



Surface Roughness Profile for Feed = 0.1 mm/rev

Figure 6 Surface Topography Constructed Through Computer Simulation

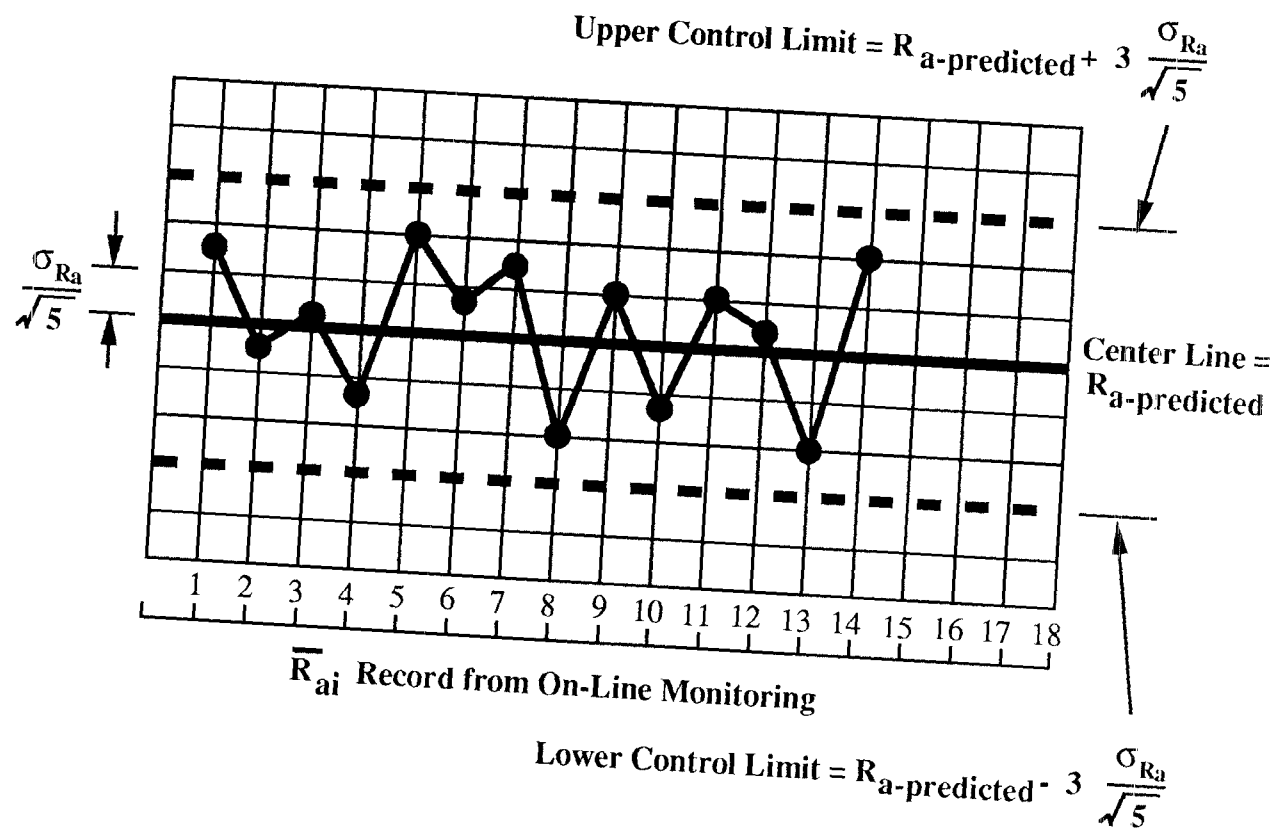


Fig. 7 \bar{R}_a - Control Chart for On-Line Monitoring

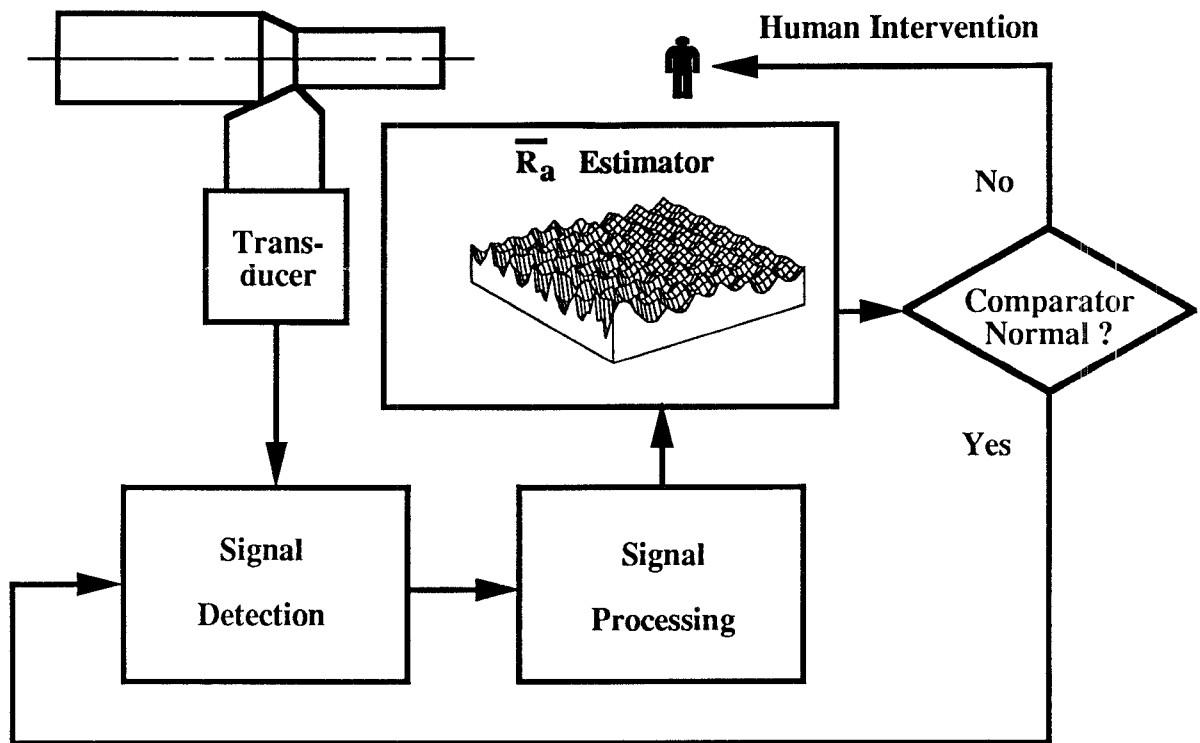


Fig. 8 Outline of the On-Line Monitoring Methodology

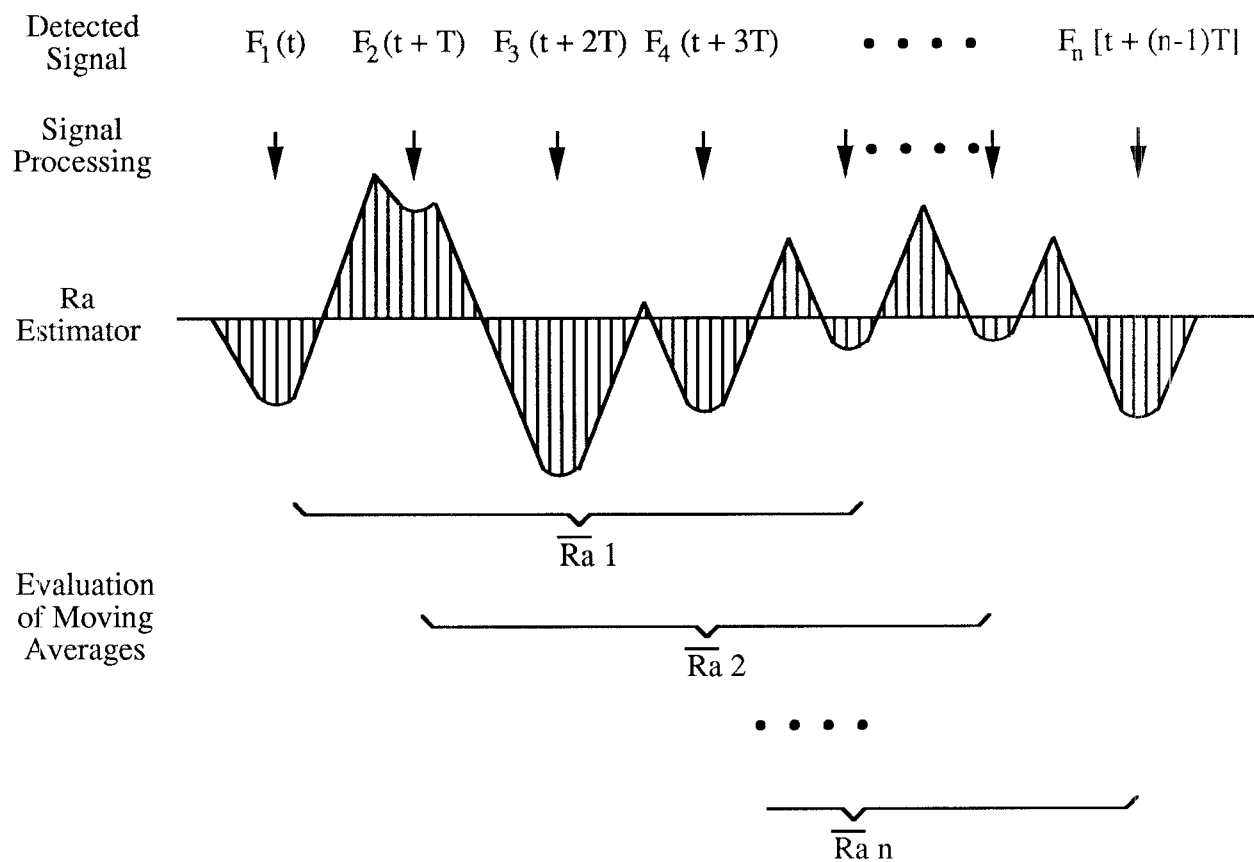


Figure 9 Evaluation of Moving Averages to Be Used on the Control Chart